





$$\omega_{spp}^2 = ck_{spp}^2 \left( \frac{\epsilon_m + \epsilon_d}{\epsilon_m \epsilon_d} \right) \quad (1.1)$$

$$k_{spp} = k_{ph} \sin \theta \pm 2\pi N / \Lambda \quad (1.2)$$

In Eq. (1.1) and (1.2),  $c$  is the speed of light in a vacuum,  $k_{spp}$  is the SPP wave vector (positive or negative depending on SPP propagation direction),  $\omega_{spp}$  is the SPP frequency,  $k_{ph} \sin \theta$  is the component of the incident light wavevector parallel to the interface,  $N$  is an integer, and  $\epsilon_m$  and  $\epsilon_d$  are the relative permittivity of the metal and dielectric materials, respectively.

For 1D periodic perturbations, such as a series of grooves, only incident light with an electric field component along the surface polarized 90 degrees to the grooves (hereafter referred to as TM polarized) can couple to SPPs [13,18]. This, along with the SPP dispersion relationship [Eq. (1.1)] and the momentum matching condition [Eq. (1.2)], sharply define the allowed polarizations and frequencies that can couple to SPPs for such geometries. The results are well-defined spectral signatures manifest in reflection measurements when the material interacts with a broadband source of light.

Selective emission from such structures has already been proposed [19–22] and experimentally verified across a range of wavelengths [16,21]. In the mid-infrared (mid-IR), Miyazaki et al., recently demonstrated selective emission from a gold film with patterned periodic nanogrooves [23,24]. The high selectivity of the observed emission peaks in ref. [23] and [24] are achieved by means of a complex, time-consuming, and costly fabrication process, which results in well-defined, high-resolution sub-wavelength features. Patterning large areas of commercially available iron or steel, and thus influencing their optical properties, could be more cost effective, and more easily developed for high-volume fabrication processes. Furthermore, as the optical properties of these metals, in the mid-IR, vary little from those used in more typical plasmonic devices [25], they can be easily incorporated into mid-IR plasmonic device designs. Finally, metals such as iron or steel have the benefit of higher thermal emissivity when compared to the gold and silver more often used for plasmonic structures [26]. Here we demonstrate, by effective wavelength-scale patterning, the ability to control the emissivity, and thus the thermal signature of commercially available steel through designed plasmonic resonances.

## 2. Fabrication and experimental set-up

For the principle experiment, 76  $\mu\text{m}$  (3 mil) thick strips of 1010 rolled carbon steel were cut and polished to reduce the surface roughness of the steel to 20 nm ( $\lambda_c/50$ ). The steel was then lithographically patterned with a photoresist etch mask and etched with a KI/I wet etch to form the ridge/groove structures. In order to allow for accurate comparison between all samples, a ridge/groove duty cycle of 50% was used for all finished emission samples. Careful selection of the initial photoresist pattern duty cycle (dependent on the desired etch depth) allowed us to compensate for undercutting of the etch mask during etching (a significant effect for deeper etches). Chemically etching the steel revealed the material's microcrystalline structure as well as imperfections in the alloy. The former showed up as surface roughness, and the latter as large and deep pits in the etched surface [Fig. 1(c)]. Because non-metallic patterned surfaces can display frequency-dependent optical properties [27,28], we also patterned a glass slide with ridge-groove structures similar to our steel samples, providing a non-metallic, mid-IR-opaque comparison sample.

The optical properties of our samples were studied in two separate experiments. Samples were first studied by reflection spectroscopy [Fig. 1(a)]. Here, normally incident broadband mid-IR light from a Bruker V70 Fourier Transform Infrared (FTIR) spectrometer was focused onto the surface of the patterned material through a mid-IR polarizer and beam splitter. Light reflected from the sample surface was collected by an external HgCdTe (MCT) detector. The TM and TE (polarized parallel to the grooves) signals were normalized to the TM and TE-

polarized reflection, respectively, from unpatterned, polished steel, and the normalized TM/TE spectra calculated. Dips in the TM/TE reflection, by Kirchoff's Law, indicate coupling to plasmonic resonances and/or un-collected diffracted light.

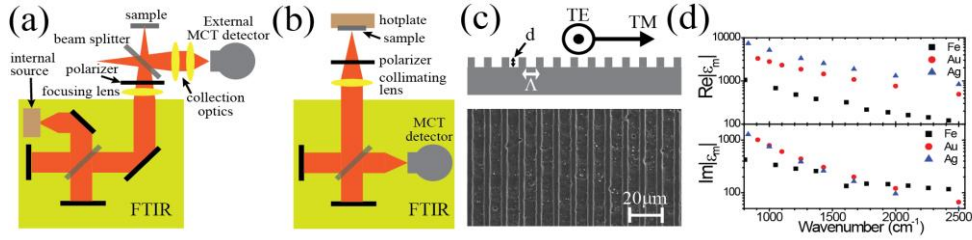


Fig. 1. Schematics of (a) reflection and (b) thermal emission setup. (c) Schematic and Scanning electron microscope image of a patterned and etched steel sample. Note the micro-crystalline roughness and pitting caused by the etching process. Coordinate system for TM,TE polarized light is indicated (d) Dielectric permittivity data used in Comsol modeling (from ref. [25]).

In the second experiment [Fig. 1(b)], the patterned sample was heated using an externally controlled and calibrated hot plate and the emission analyzed with the FTIR spectrometer. Heating of the steel is expected to alter the dielectric permittivity function of the material [29], however, in the mid IR, most metals have a large negative permittivity [Fig. 1(d)] and such a change can have very little effect on the optical properties of the metal/dielectric structure [Eq. (1.1)]. A polarizer was used to distinguish between the TM and TE polarized thermal radiation. After background subtraction from the emission spectra for each polarization, the background corrected TM/TE ratio was calculated, giving a measure of the intensity enhancement of the TM polarized emission from the sample surface. A sample temperature of 200 °C was chosen to give a thermal emission signal intense enough to be clearly seen above the background, but still low enough to prevent oxidation of unprotected steel samples. Our emission data, unlike the reflection data (which gives the sum of the absorbed and diffracted light), is a direct measure of the selective emissivity (and thus absorption) of our structures.

The selective coupling of incident light to propagating surface waves on our patterned steel was numerically modeled using the COMSOL Multiphysics simulation software [Fig. 1(c)] using the Iron permittivity data of ref. [25] [Fig. 1(d)]. In the model, the patterned steel surface was illuminated, at normal incidence, by light of varying wavelengths in both TM and TE polarizations. The strength of the coupling to these surface waves was determined by measuring power flow across the surface of the steel away from the source beam. The modeled wavelength-dependent in-coupling accurately mirrors the wavelength-dependent out-coupling of thermally generated surface waves to normally emitted light, effectively providing us with numerical simulations of the selective emission phenomenon we are investigating.

Finally, using a FLIR BX320 camera with a vanadium oxide micro bolometer focal plane array (with 8 mK resolution and 13ms reaction time) and a polarizer, we took images of a 100°C steel sample heated on the same hot plate used for emission measurements. The FLIR camera returns the integrated intensity over a spectral range of 770  $\text{cm}^{-1}$  to 1300  $\text{cm}^{-1}$  (7.5-13  $\mu\text{m}$ ), encompassing the first resonant selective emission peak at 1000  $\text{cm}^{-1}$ . Images were taken of the TM polarized emission and the TE polarized emission and visually compared.

### 3. Results and conclusions

Representative normalized reflection and emission spectra are shown in Fig. 2(a). As expected, the reflection spectra for the patterned steel reveals absorption resonances at 1000  $\text{cm}^{-1}$  and 2000  $\text{cm}^{-1}$ , corresponding to the first two SPP resonant coupling frequencies ( $N = 1, 2$ ) for a 10  $\mu\text{m}$  periodicity pattern [Eq. (1.2)]. The resonances seen in each of the samples' reflection spectra aligned spectrally with the emission resonance in the corresponding samples' emission, as predicted by Kirchoff's Law. As the optics of the

reflection setup only capture normally reflected light, the high energy tail extending from the 10  $\mu\text{m}$  reflection resonance dip is attributed to light which is not coupled to surface waves and then absorbed, but is instead diffracted from the surface (neither collected, not absorbed). For the emission spectra, the peak value of the TM/TE resonance at 1000  $\text{cm}^{-1}$  gives the selectivity of the thermal emission from the sample. All of the patterned samples showed resonant reflection/emission peaks at 1000  $\text{cm}^{-1}$ . However, a large variation in the emission enhancement was observed, ranging from TM peak values 3% to 160% greater than the TE polarized emission at the same wavelength [Fig. 2(b)].

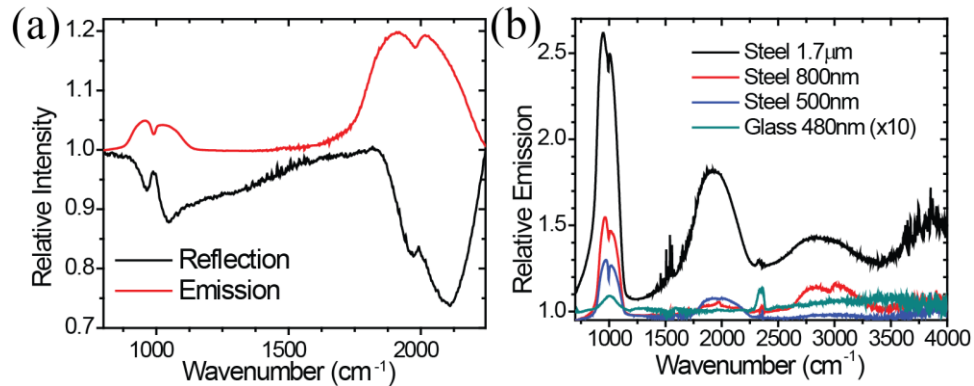


Fig. 2. (a) TM/TE reflection (black) and 200 °C TM/TE emission (red) spectra of a 1  $\mu\text{m}$  deep patterned steel sample. (b) Background-corrected TM/TE emission spectra at 200 °C for chemically etched steel and etched glass (x10) with various groove depths and 10  $\mu\text{m}$  periodicity.

The patterned glass slide showed detectable selective thermal emission at the target wavenumber of 1000  $\text{cm}^{-1}$  indicating that plasmonic effects are not the only means of selective emission in periodic structures. However, the selective emission from the glass substrate was a factor of 3 weaker than the weakest selective emission from a patterned steel sample and thirty times weaker than selective emission from steel samples with comparably deep grooves [Fig. 2(b)]. This result, supported by the calculations of ref. [20], suggests that our structure's ability to support surface waves, not the structure's geometry, plays the dominant role in the selective emission observed in our patterned steel samples.

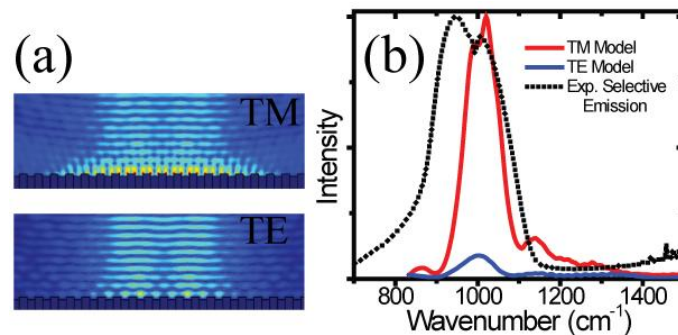


Fig. 3. (a) Numerically modeled electric field intensity for light normally incident on a patterned steel surface (10  $\mu\text{m}$  period). (b) Normalized time averaged power flow at the metal/air interface measured 50  $\mu\text{m}$  from the edge of the incident beam as a function of wavelength for TM (red) and TE (blue) polarized light. Peak selectivity for the modeled structure is a factor of  $\sim 5$  stronger than our largest experimentally observed selectivity (presumably due to the fabrication-related damage to the steel surface).

Contour plots, generated by the Comsol simulations of our structures, of the electric field intensity at and above the structure surface for incident light at  $10\mu\text{m}$ , are shown in Fig. 3(a) for both TM and TE polarized light. For the TM light, a clear coupling to surface waves is observed, with a strong electric field at the sample surface (penetrating  $\sim 20\text{nm}$  into the steel), and power flow propagating away from the incident beam, along the sample surface. The spectra in Fig. 3(b) shows the modeled power flow along the steel surface as a function of wavelength, for both TM (red) and TE (blue) polarizations, compared to the normalized selective emission from one of our samples. The experimental data shows a somewhat broadened linewidth, which is to be expected given the pitting and other fabrication-related non-uniformities observed on our sample surfaces [Fig. 1(c)]. However, apart from the expected broadening, the modeled surface wave propagation and the experimentally determined emission enhancement show good agreement, further suggesting the important role played by these propagating surface waves in the thermal emission characteristics of our devices.

Selectivity of the thermal emission of our samples showed a strong dependence on groove depth. Steel samples were fabricated with groove depths ranging from  $107\text{ nm}$  to  $2.7\ \mu\text{m}$  and TM/TE emission enhancement at  $200^\circ\text{C}$  was recorded for each sample at the designed resonance of  $1000\text{ cm}^{-1}$ . A somewhat broad range of enhancement data for similar groove depths was observed, due most likely to variations between samples in etch quality. Nonetheless, a general trend in the data may be discerned [Fig. 4(a)]. The emission enhancement of the patterned steel samples increased as much as a factor of sixty between groove depths of  $107\text{ nm}$  and  $2\ \mu\text{m}$ . Enhancement decreases drastically with deeper etches, indicating an optimum etch depth for enhancing the coupling of SPP modes to free space photons. Previous studies have seen similar trends with groove depth, attributed to the geometry-dependent resonant excitation of cavity modes in the subwavelength grooves [23]. Our samples, however, do not have nearly the geometric precision of these works. It is more likely, for this work, that the decrease in selectivity beyond a certain groove depth is the result of the increased etch damage seen in the samples with the deepest grooves. With these production methods, therefore, deeper etching is expected to produce greater damage and reduced selectivity.

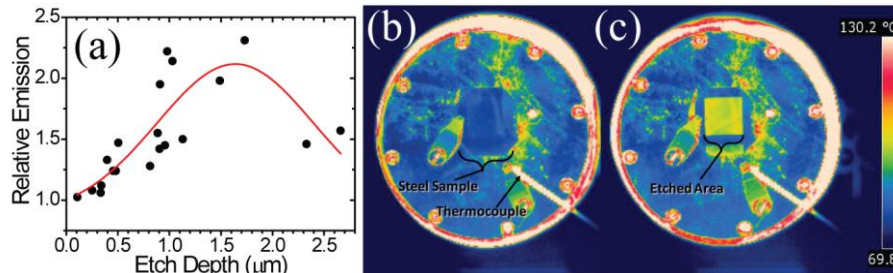


Fig. 4. (a) Emission selectivity at  $1000\text{ cm}^{-1}$  as a function of groove depth, with a fit line indicating an optimal groove depth for selective thermal emission relative intensity. (b) TE polarized and, (c) TM polarized thermal image of patterned and chemically etched steel at  $100^\circ\text{C}$ . The polarized, enhanced emission is clearly visible in the TM polarized image. Note that the temperature scale is calibrated to objects with an emissivity of 0.1. The scale does not indicate the surface temperature of the steel and is provided as a reference only.

Images of thermal emission were collected with a FLIR infrared camera. Despite the broad ( $7.5\text{-}13\ \mu\text{m}$ ) response of the camera, the selectivity of the emission at  $1000\text{ cm}^{-1}$  was clearly observed simply by switching the polarization of the detected light [Fig. 4(b) and 4(c)]. These images show a clear emission enhancement for TM-polarized thermal radiation.

The above results demonstrate strongly selective thermal emission from directly patterned steel substrates. Furthermore, comparison of experimental reflection and emission data to our numerical modeling convincingly suggests that this selective emission is due to the excitation of surface plasmons and their coupling to free space photons at the metal/dielectric interface.

Future work that models the effect of a rough and pitted surface on selective plasmon coupling may prove to be beneficial for the development of scalable and affordable plasmonic devices, based on commercially available, cost effective metals. The abundance and low cost of steel, and the ability to directly pattern the steel with subwavelength features, makes for a cost effective manufacturing process. The work presented here demonstrates the possibility of low-cost, large-area processing of metal films for control of the materials' optical properties, specifically, the thermal radiation signatures of structures coated with these materials.